Talanta 114 (2013) 54–59

Contents lists available at ScienceDirect

Talanta

journal homepage: www.elsevier.com/locate/talanta

Graphene matrix for signal enhancement in ambient plasma assisted laser desorption ionization mass spectrometry

Cuilan Chang, Xianjiang Li, Yu Bai*, Gege Xu, Baosheng Feng, Yiping Liao, Huwei Liu*

Beijing National Laboratory for Molecular Sciences, the Key Laboratory of Bioorganic Chemistry and Molecular Engineering of Ministry of Education, Institute of Analytical Chemistry, College of Chemistry and Molecular Engineering, Peking University, Beijing 100871, China

ARTICLE INFO

Article history:
Received 14 December 2012
Received in revised form
26 March 2013
Accepted 4 April 2013
Available online 12 April 2013

Keywords:
Ambient PALDI-MS
Graphene
α-cyano-4-hydroxycinnamic acid
Graphene oxide
Signal enhancement

ABSTRACT

In this work, the signal intensity of ambient plasma assisted laser desorption ionization mass spectrometry (PALDI-MS) was significantly increased with graphene as matrix. The graphene functions as a substrate to trap analytes, absorb energy from the visible laser irradiation and transfer energy to the analytes to facilitate the laser desorption process. The desorbed analytes are further ionized by helium plasma and analyzed by MS. Compared with a traditional organic matrix, α-cyano-4-hydroxycinnamic acid (CHCA), graphene exhibited much higher desorption efficiency for most of the compounds benefitting from the strong optical absorption at 532 nm. The performance has been confirmed by the facile analysis of more than forty compounds with various structures. Additionally, this method was successfully applied to distinguish three kinds of Chinese tea leaves by detecting the endogenous caffeine and theanine, which proved the utility, facility and convenience of this method for rapid screening of main components in real samples.

1. Introduction

Direct analysis in real time mass spectrometry (DART-MS) [1], which is operated in the open air conditions and requires minimal or no sample preparation, is one of the most widely used ambient mass spectrometry. Helium or nitrogen metastable plasma is created by high-voltage glow discharging. Then the heated plasma blows to the sample surface, and the protons are transferred to analytes through the reactive species in the ambient atmosphere, such as water clusters [1,2]. DART-MS could provide a rapid and direct way to analyze many kinds of samples, such as direct analysis of activity assays from live samples [3,4], fast screening of target compounds in real samples [5–7], obtaining evidence of sexual assaults [8], reaction monitoring in drug discoveries [9], quantitative detections of warfare agents [10], and efficient analysis of environmental samples after stir bar absorptive extraction [11]. Since DART is a plasma-based ambient ionization source, the desorption area depends on the plasma stream with several millimeters in diameter, which prevents its utilization for mass spectrometry imaging. The improvement of the spatial resolution can be achieved by using laser desorption and plasma assisted ionization process [12]. Based on these, our lab constructed an ambient plasma assisted laser desorption ionization mass spectrometry (PALDI-MS) system [13], and the previous results indicated that using a proper matrix to enhance the laser desorption process will definitely improve the signal intensity and detection sensitivity [14]. However, little attention has been paid to look for such matrices in laser based ambient MS [14–16].

Graphene has attracted increasing interests because of its outstanding properties since Novoselov and Geim et al. succeeded in preparing single-layer graphene in lab by simple mechanical exfoliation in 2004 [17]. This single atom thick and two-dimensional nanomaterial possesses large surface area (2630 m^2/g), excellent optical absorption and super electrical properties. With the inherent superiorities, graphene was considered as a prominent material in energy absorption, storage and transfer [18–21]. Recently, graphene-based nanomaterials have been successfully used as matrices in MALDI-ToF-MS for the detections of small molecules without matrix interferences [22–27]. So far, there is no report on the matrix effects of graphene in laser desorption process under ambient conditions.

In this study, graphene was used as the matrix to increase the signal intensity of PALDI-MS. Since graphene has large surface area and strong optical absorption across the visible range, it could not only adsorb the analyte molecules, but also act as an excellent medium to transfer the energy of laser irradiation to the analytes. The efficient energy absorption and transfer facilitate the desorption process, thus enhancing the signal intensity of MS. Owing to its superiority in interaction with analytes and visible laser absorption, homogeneous sample layer can be formed after the addition of graphene, and a higher desorption efficiency for most of the compounds has been presented when compared with a traditional matrix CHCA. In addition, the matrix effects of graphene oxide have also been investigated because it has similar π-conjugated structure with graphene. Graphene oxide exhibited considerable signal enhancement for PALDI-MS as

* Corresponding authors. Tel.: +86 10 62754976; fax: +86 10 62751708.
E-mail addresses: yu.bai@pku.edu.cn (Y. Bai), hwliu@pku.edu.cn (H. Liu).

0039-9140/$ - see front matter © 2013 Elsevier B.V. All rights reserved.
http://dx.doi.org/10.1016/j.talanta.2013.04.007

well, but not as high as graphene, which may result from its polar moieties. The performance was confirmed by the facile analysis of more than forty compounds with various structures, which demonstrated that graphene was a more general and effective matrix for ambient PALDI-MS. Finally, we used this method to analyze three kinds of Chinese teas and successfully distinguished them by the different contents of their endogenous caffeine and theanine, which proved the applicability of this method for real samples.

2. Experimental

2.1. Chemicals and reagents

Graphene aqueous suspension (0.5 mg/mL) and graphene oxide powder were obtained from Nanjing XFNANO Materials Tech Co., Ltd. (Jiangsu, China). CHCA was purchased from Sigma-Aldrich (St. Louis, MO, USA). HPLC grade methanol and purified water were obtained from Dikma Technologies Inc. (CA, USA) and Hangzhou Wahaha Group Co., Ltd. (Zhejiang, China), respectively. Model compounds without special declaration were all obtained from commercial source, and they were used in the experiments without further purification.

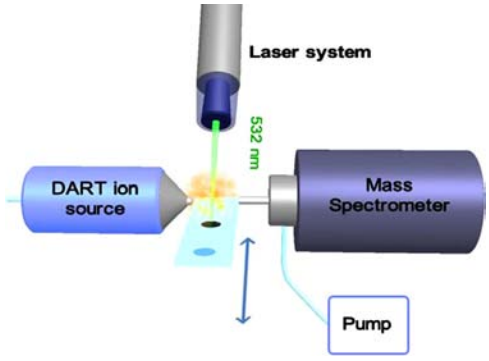

Fig. 1. Schematic illustration of the plasma assisted laser desorption ionization mass spectrometry (PALDI-MS).

2.2. Sample preparation for analysis

All of the model compounds without additional comments were dissolved in methanol and prepared at the concentration of 1.0 mg/mL. Graphene oxide powder (3.0 mg) was dispersed in 6 mL water and sonicated for 5 min to obtain homogeneous graphene oxide suspension at the concentration of 0.5 mg/mL.

Graphene and graphene oxide suspensions were sonicated for 3 min before use. Sample solutions were prepared by mixing the analyte solutions with water, graphene, CHCA or graphene oxide suspensions (1:1, v/v), respectively. The final concentration of the model compounds were 0.5 mg/mL. After sonication for 3 min, 5.0 μL solutions were dropped onto the sample plate and dried in the open air for further analysis.

2.3. Apparatus

The schematic illustration of the setup was shown in Fig. 1. The PALDI-MS system successfully integrated the visible laser ablation, the excited plasma from direct analysis in real time (DART) and Time-of-Flight MS (ToF MS). The DART®-SVP ion source (IonSense, Saugus, MA, USA) was coupled to an Agilent MSD ToF MS (Agilent Technologies, Palo Alto, CA, USA) after removing the Agilent dual electrospray ionization source. The pulsed Nd:YAG laser (Lai Yin Opto-Electronics Technology, Beijing, China) was operated at 532 nm

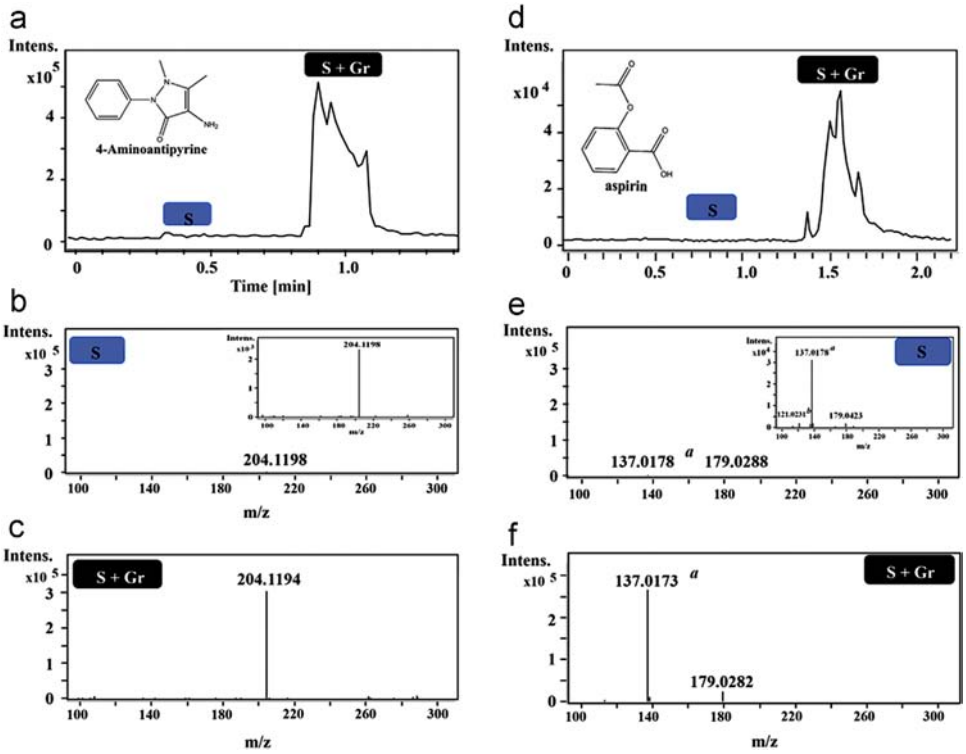

Fig. 2. Mass spectra of 4-aminoantipyrine and aspirin under 532 nm of laser without/with graphene as the matrix. (a) EIC of 4-aminoantipyrine (*m*/*z*, 204.1131) in positive ion mode; (b) averaged mass spectrum of 4-aminoantipyrine without matrix (inlet is the amplified average mass spectrum); (c) averaged mass spectrum of 4-aminoantipyrine with graphene as the matrix; (d) EIC of aspirin (*m*/*z*, 137.0178) in negative ion mode; (e) averaged mass spectrum of aspirin without matrix (inlet is the amplified average mass spectrum); (f) averaged mass spectrum of aspirin with graphene as the matrix.

with a pulse length of 10 ns at 10 Hz and impinged the sample surface with quasicircular focal spots of approximate 250 μm. The angle between the laser beam and sample plate was kept at 45°. In optimized configuration, the sample plate was placed approximately 3 mm lateral offset of the plane of DART and ion transfer tube; the distance between DART and ion transfer tube was 10 mm; the distance between the DART ion source and sample plate was 2 mm. An x,y,z-robotic platform (STEP Motion Control System Engineering Co., Ltd., Shanghai, China) with a home-made sample plate holder, was used to manipulate the position of the sample plate. It was moved at the rate of 0.5 mm/s during data acquisition to ensure fresh sample area was probed for each pulse. DART ion source was operated at room temperature; the discharge needle voltage, grid voltage and helium flow rate were set at 6000 V, 80 V and 2 L min^{-1}, respectively. The MS-related parameters were set as follows: capillary voltage −3500 V/+3500 V, drying gas temperature at 325 °C and drying gas flow rate at 5 L min^{-1}. The MS data were acquired at a rate of 1.00 spectra s^{-1} in the range of *m/z* 50–800 by MassHunter Data Acquisition B.02.00 (Agilent Technologies, CA, USA) and analyzed with MassHunter Qualitative Analysis B.02.00 (Agilent Technologies, CA, USA).

2.4. Characterizations of graphene and graphene oxide

Graphene and graphene oxide were characterized by scanning electron microscopy (SEM, Hitachi, S4800, 1 kV, Tokyo, Japan) (Fig. S1 and S2), atomic force microscopy (AFM, Veeco/DI, NanoscopeIII(a), tapping mode, Santa Barbara, CA, USA) (Fig. S3 and S4), and UV–vis absorption spectroscopy (Fig. S5). The results demonstrated the single layer structure of graphene and graphene oxide, which could provide large surface area to trap the analyte molecules and act as energy receptacle for laser irradiation.

2.5. Preparation of Chinese tea samples

For each kind of the Chinese tea, 2 g leaves were mixed with 10 mL 90 °C H_2O and ultrasonically extracted for 20 min. Then, the three extracts were detected on PALDI-MS using graphene as the matrix.

3. Results and discussion

3.1. Matrix effects of graphene

In the experiments, the samples without matrix (defined as "S") were first dropped onto the sample plate and followed by samples with graphene as matrix (defined as "S+Gr"). These samples were scanned sequentially. 4-Aminoantipyrine was taken as an example for the detection on positive ion mode. As shown in Fig. 2, the differences of the two samples were easily distinguished (Fig. 2a–c). Apparently, regular lanes with the width of approximately 250 μm were found from "S+Gr" after laser irradiation (Fig. S6). The extracted ion chromatograms (EICs) of 4-aminoantipyrine ($[M+H]^+=204.1131$) obtained without or with graphene were shown in Fig. 2b. When the laser irradiated "S", the signal was so weak that it even could not

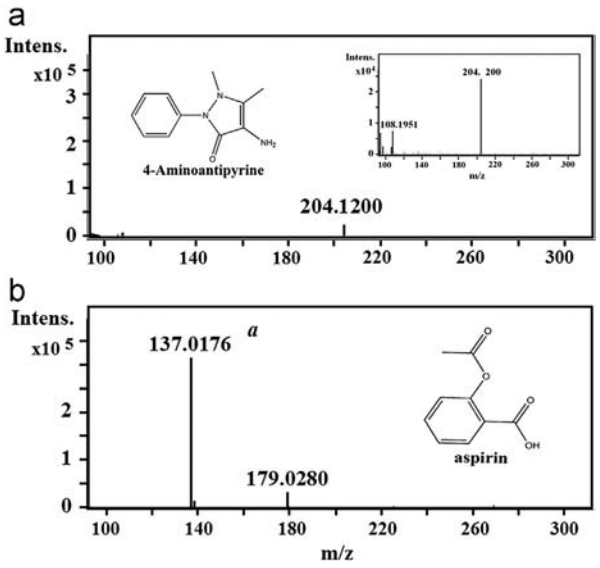

Fig. 4. Mass spectra of 4-aminoantipyrine and aspirin under 532 nm laser irradiation with CHCA as the matrix. (a) EIC of 4-aminoantipyrine (*m/z*, 204.1131) in positive ion mode; (b) EIC of aspirin (*m/z*, 137.0178) in negative ion mode.

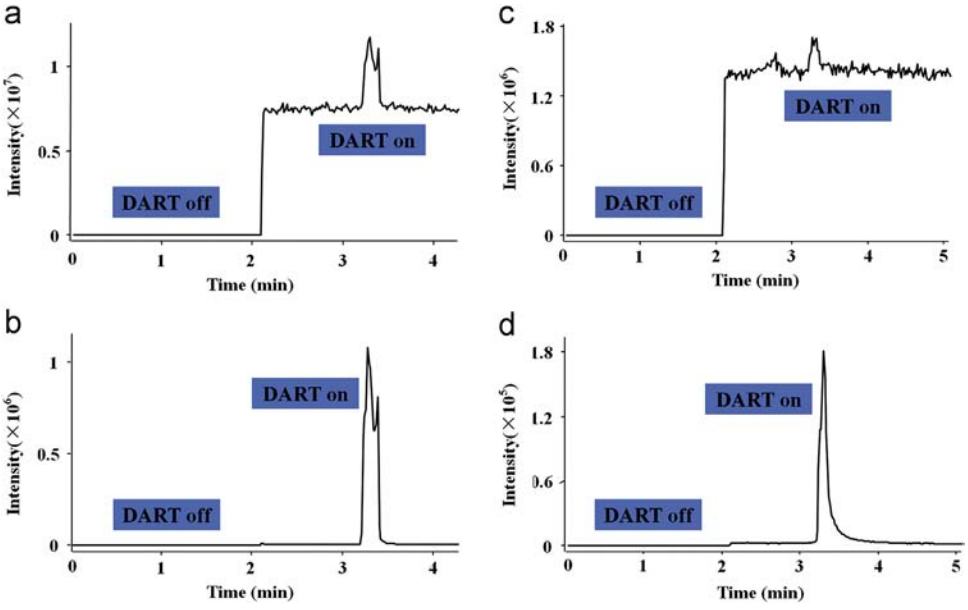

Fig. 3. Study of the laser desorption process. (a) TIC of 4-aminoantipyrine under "off" or "run" mode; (b) EIC of 4-aminoantipyrine under "off" or "run" mode; (c) TIC of tetradecanoic acid under "off" or "run" mode; (d) EIC of tetradecanoic acid under "off" or "run" mode.

be detected; while once the laser impinged on "S+Gr", the signal intensity increased dramatically. The signal-to-noise ratio (S/N) increased from 13 to 352 after the addition of graphene as matrix. After repeating the process for at least six times, we confirmed that graphene was able to increase the signal intensity of PALDI-MS (532 nm) when it was used as matrix. Under negative ion mode, aspirin ($[M-H]^- = 179.0342$, $[M-COCH_3]^- = 137.0178$) showed the same tendency (Fig. 2d–f). We propose that graphene functions to trap the analyte molecules and acts as an energy receptacle for laser irradiation [22]. Due to its large surface area of its nanosheet structure, graphene could attach to the target molecules more tightly and form homogeneous suspension. Therefore, samples with graphene as the matrix could form more uniform layer on the sample plate (Fig. S6) and improve the reproducibility. In addition, the monolayer structure with large surface area can provide efficient energy transfer between the analyte and graphene, and improve the desorption ability of the analyte from graphene, thereby enhancing the MS signal. Although linear range has not been thoroughly studied, the detection of 0.4 ng 4-aminoantipyrine still indicated the high sensitivity of the ambient PALDI-MS when using graphene as the matrix.

The ionization mechanism of the PALDI-MS system was discussed a little in previous report [13]. As mentioned before, in this system, DART source is utilized to produce the helium plasma and laser is applied mainly for the analyte desorption. When DART was put on "run" mode, helium plasma was produced and the laser desorbed analytes were ionized; while when it was put on "off" mode, no helium plasma was generated, and the MS would only record the signal of laser induced ionized species. The contrast experiments were carried out using 4-aminoantipyrine as the model compound on positive mode to study more about the matrix effects of graphene. Firstly, DART was put on "off" mode (0–2 min in Fig. 3a and b), and the signals were too low to be detected in the total ion chromatograms (TICs) and EICs. When DART was put on "run" mode (2–4 min in Fig. 3a and b), the signals were increased greatly. Comparing with that in vacuum, the low ionization efficiency of graphene in the ambient conditions may due to the fact that there were more interferences and less effective ion transferring. Similar results were obtained when using tetradecanoic acid on negative mode (Fig. 3c and d). Therefore, we proposed that the main contribution of graphene in ambient PALDI-MS was to promote the analyte desorption through the

Table 1
Various molecules with different chemical structures detected by using PALDI-MS (532 nm).

Ion mode	Samples	Molecular weight	Detected *m/z*	S/N			
				S	S+CHCA	S+GO	S+Gr
Positive	4-Aminoantipyrine	203.1059	204.1125	13	23	50	352
	Anthranone	194.0732	195.0799	77	146	202	285
	Benzanilide	197.0841	198.0902	103	104	247	548
	Acridine	179.0735	180.0801	75	68	108	131
	4-Nitroaniline	138.0429	139.0500	30	137	271	1079
			156.0762[a]	56	219	381	1464
	Benzoin	212.0837	213.0901	87	206	409	599
			230.1168[a]	246	517	1188	1677
	1-Benzoylnaphthalene	232.0888	233.0952	36	118	205	382
			250.1219[a]	116	121	196	348
	N-(3-acetyl-4-hydroxy-phenyl)butyramide	221.1052	222.1120	< 1	< 1	224	155
			239.1382[a]	< 1	< 1	402	260
	Metronidazole	171.0644	172.0710	< 1	32	283	650
	Progesterone	314.2246	315.2312	< 1	15	327	1231
	Methyltestosterone	302.2236	303.2319	< 1	167	260	335
	Artemisinin	282.1467	300.1805[a]	< 1	68	1003	1694
	Quinine	324.1838	325.1919	< 1	< 1	147	210
	Acetaminophen	151.0633	152.0700	< 1	< 1	180	521
	Amitriptyline	277.1830	278.1899	< 1	< 1	97	137
	Caffeine	194.0804	194.0871	< 1	< 1	663	1095
	n-Octadecylamine	269.3083	270.3152	< 1	< 1	315	1741
	Theophylline	180.0647	181.0713	< 1	< 1	9	34
	4-Amino-3,5-dimethyl-1,2,4-triazole	112.0749	113.0814	< 1	< 1	2490	5079
negative	Aspirin	180.0423	179.0342	11	4	825	778
			137.0178[b]	25	7	610	584
	p-Chlorobenzoic acid	155.5592	154.9901	128	816	1929	1878
			156.9898	72	645	1717	1658
	o-Nitrobenzoic acid	167.0219	166.0147	492	469	1699	3283
	m-Nitrobenzoic acid	167.0219	166.0144	281	611	665	966
	p-Nitrobenzoic acid	167.0219	166.0143	180	317	366	424
	α-Naphthoic acid	172.0524	171.0446	3	20	1499	1603
	Carbazole	167.0735	166.0655	3	3	81	121
	Barbituric acid	128.0222	127.0141	< 1	11	125	360
	Hippuric acid	179.0582	178.0501	< 1	4	178	1056
	m-Hydroxybenzoic acid	138.0317	137.1238	< 1	91	786	1617
	2, 5-Dihydroxy benzoic acid	154.0266	153.0187	< 1	29	674	746
	3,5-Dinitrosalicylic acid	228.0019	226.9957	< 1	13	267	295
	Dodecanoic acid	200.1778	199.1701	< 1	< 1	649	704
	Tetradecanoic acid	228.2089	227.2011	< 1	< 1	283	561
	Hexadecanoic acid	256.2402	255.2322	< 1	< 1	106	484
	Octadecanoic acid	284.2715	283.2636	< 1	< 1	45	33
	Arachidic acid	312.3028	311.2951	< 1	< 1	19	26
	Decanedioic acid	202.1205	201.1127	< 1	< 1	1249	1709
	Erucic acid	338.3185	337.3101	< 1	< 1	1275	3125

[a] $[M+NH_4]^+$.
[b] $[M-COCH_3]^-$.

effective absorption and transfer of the laser energy, and thus increase the MS intensity as soon as the desorbed species fused with metastable helium plasma produced by DART.

3.2. Comparison with CHCA

CHCA is one of the most widely used organic matrices in MALDI-MS analysis. In this work, we compared the matrix effects of graphene with CHCA. The mass spectrum of 4-aminoantipyrine with CHCA as the matrix (defined as "S+CHCA") was shown in Fig. 4a with the signal intensity of ~4.2 × (10∧3), which was almost equal to that of sample without matrix [~2.3 × (10∧3)]. Compared with graphene [signal intensity of ~3.2 × (10∧5)], CHCA did not show obvious signal enhancement for 4-aminoantipyrine. The same tendency was also obtained under negative ion mode using aspirin as the model compound (Fig. 4b). It was proposed that the weak matrix effects were due to the low absorption efficiency of CHCA under visible laser irradiation. As is well known, the maximum absorption wavelength of CHCA was in ultraviolet, and its absorption at 532 nm was much weaker than that of graphene. When CHCA was used as the matrix, it desorbed much fewer species under visible laser irradiation than graphene. Therefore, the signal enhancement of CHCA was not as remarkable as that of graphene. To some extent, graphene could be regarded as a more effective matrix than traditional CHCA for ambient PALDI-MS when using visible laser for irradiation.

3.3. Analysis of other small molecules

In order to confirm whether graphene could be regarded as a general matrix to increase the signal intensity of small molecules when using visible laser irradiation, various compounds with different structures were tested under positive or negative ion mode, such as straight chain compounds like *n*-octadecylamine, cyclic compounds like methyl testosterone, aromatic compounds like 2, 5-dihydroxy benzoic acid, and large conjugated systems like anthranone. The results shown in Table 1 demonstrated that graphene could greatly improve the sensitivity for all the compounds regardless of their structures. For example, the S/N of *n*-octadecylamine ($[M+H]^+$, *m*/*z* 270.3152) and dodecanoic acid ($[M-H]^-$, *m*/*z* 199.1701) reached as high as 1741 and 704, respectively, whereas the S/N were smaller than 1 when there was no graphene. Similar results were also observed for cyclic compounds, aromatic compounds and large conjugated systems. The matrix effects of CHCA were also investigated using the same model compounds. The results demonstrated that CHCA did not have obvious signal enhancement under visible laser irradiation for most of the compounds.

Usually, graphene is considered to be non-polar and hydrophobic, while graphene oxide, containing polar moieties, such as hydroxy, epoxy, and carboxy groups, is considered to be more polar and hydrophilic than graphene [28]. Compared with graphene, graphene oxide has similar π-conjugated structure but different functional groups. In our work, the matrix effect of graphene oxide was also studied to assist the understanding of the graphene matrix. The samples with graphene oxide as the matrix were defined as "S+GO". Interestingly, graphene oxide also showed good signal enhancement for the model compounds in most cases, such as benzoin, artemisinin, caffeine, m-nitrobenzoic acid and m-hydroxybenzoic acid, but not as remarkable as graphene. This could be explained by the facts: (1) compared with graphene, the same concentration of graphene oxide shows weaker absorption at 532 nm (Fig. S5); (2) the residual polar groups enable the formation of hydrogen bond and electrostatic interactions between graphene oxide and model compounds besides the π–π stacking interaction [29,30], which hindered the species desorbing from the matrix. The above reasons resulted in lower ionization efficiency of graphene oxide than that of graphene, and indicated that graphene could be regarded as a more general and effective matrix for the signal enhancement under visible laser irradiation.

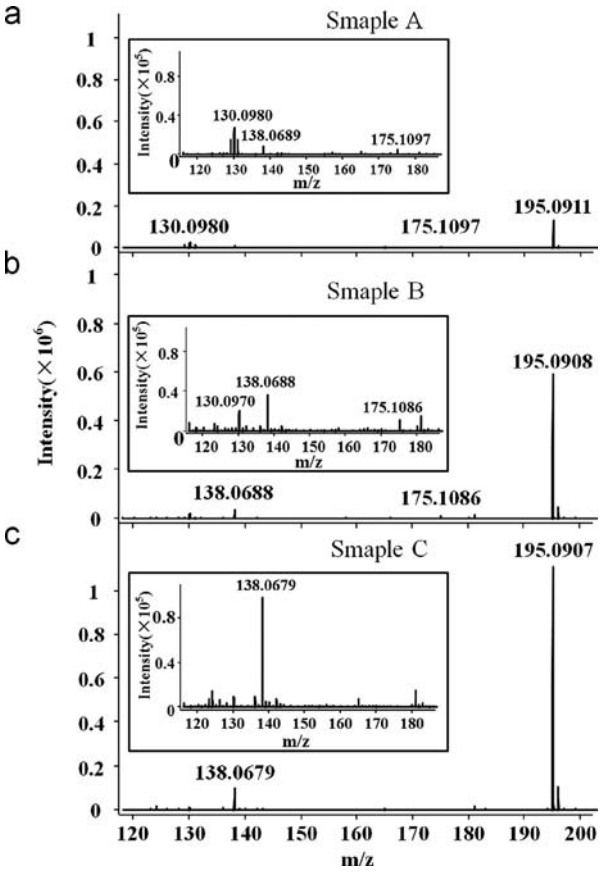

Fig. 5. Mass spectra of Chinese Tea using PALDI-MS. See Experimental section for other conditions. (a) average mass spectrum of sample A; (b) average mass spectrum of sample B; (c) average mass spectrum of sample C (insets were the enlarged views).

3.4. Applications for real samples

Caffeine and theanine are the two main components in Chinese tea, and their contents are closely related to the grade and quality of the tea. Due to the various production processes of Chinese tea, the amounts of the main components in the tea leaves may have some differences. In our experiments, we detected the endogenous caffeine and theanine in three types of Chinese tea (defined as sample A, B and C). The extracts of the three kinds of Chinese tea were directly mixed with graphene without further preparation and then detected using PALDI-MS. The average mass spectra obtained on positive mode were shown in Fig. 5a–c, respectively. The peaks of *m*/*z* 195.0880 and 175.1077 were corresponding to endogenous caffeine and theanine, while 138.0672 and 130.1111 were attributed to the loss of the CH_3NCO or COOH groups from caffeine and theanine, respectively. As Fig. 5a–c showed, the contents of caffeine increased from sample A to C. From the insets in Fig. 5a–c, we can see that the content of theanine in sample B is the highest, followed by sample A, and it was hard to observe theanine in sample C. In summary, these results showed the differences of the three Chinese teas and proved the utility, facility and convenience of this method for rapid screening of main components in real samples.

4. Conclusions

The capability of graphene matrix in ambient PALDI-MS for the analysis of small molecules was investigated. The experimental results showed that graphene matrix can increase the signal intensity and improve the reproducibility in ambient PALDI-MS. The main contribution of graphene in ambient PALDI-MS was to promote the analyte desorption through the effective absorption and transfer of the laser energy, and thus increase the MS intensity as soon as the desorbed species fused with metastable helium plasma produced by DART. The matrix effects were further confirmed by the facile analysis of more than forty compounds with different chemical structures, such as straight chain compounds like *n*-octadecylamine, cyclic compounds like methyl testosterone, aromatic compounds like 2, 5-dihydroxy benzoic acid, and large conjugated systems like anthranone. The comparison with CHCA and graphene oxide demonstrated that graphene was more general and effective for signal enhancement in ambient PALDI-MS. In addition, the successful detection of varying contents of endogenous caffeine and theanine were performed in the distinction of the quality and grade of Chinese teas, which proved the utility, facility and convenience of this method for rapid analysis of real samples. It is expected that, with the assist of different novel matrix, our experiments can provide a high sensitive target screening approach in the open air as well as complementary information for the comprehensive understanding of the graphene matrix-effects.

Acknowledgments

This work was financially supported by the National Natural Science Foundation of China (Grant nos. 21027012, 21275012 and 91132717) and the Fundamental Research Funds for the Central Universities.

Appendix A. Supporting information

Supplementary data associated with this article can be found in the online version at http://dx.doi.org/10.1016/j.talanta.2013.04.007.

References

[1] R.B. Cody, J.A. Laramee, H.D. Durst, Anal. Chem. 77 (2005) 2297–2302.
[2] J.L. Rummel, A.M. McKenna, A.G. Marshall, J.R. Eyler, D.H. Powell, Rapid Commun. Mass Spectrom. 24 (2010) 784–790.
[3] V.L.H. Bevilacqua, J.M. Nilles, J.S. Rice, T.R. Connell, A.M. Schenning, L.M. Reilly, H.D. Durst, Anal. Chem. 82 (2010) 798–800.
[4] J.Y. Yew, R.B. Cody, E.A. Kravitz, Proc. Nat. Acad. Sci. USA 105 (2008) 7135–7140.
[5] Z.G. Zhou, J.L. Zhang, W. Zhang, Y. Bai, H.W. Liu, Analyst 136 (2011) 2613–2618.
[6] C.S. Deroo, R.A. Armitage, Anal. Chem. 83 (2011) 6924–6928.
[7] R.B. Cody, A.J. Dane, B. Dawson-Andoh, E.O. Adedipe, K. Nkansah, J. Anal. Appl. Pyrol. 95 (2012) 134–137.
[8] R.A. Musah, R.B. Cody, A.J. Dane, A.L. Vuong, J.R.E. Shepard, Rapid Commun. Mass Spectrom. 26 (2012) 1039–1046.
[9] C. Petucci, J. Diffendal, D. Kaufman, B. Mekonnen, G. Terefenko, B. Musselman, Anal. Chem. 79 (2007) 5064–5070.
[10] J.M. Nilles, T.R. Connell, H.D. Durst, Anal. Chem. 81 (2009) 6744–6749.
[11] M. Haunschmidt, C.W. Klampfl, W. Buchberger, R. Hertsens, Anal. Bioanal. Chem. 397 (2010) 269–275.
[12] A.S. Galhena, G.A. Harris, L. Nyadong, K.K. Murray, F.M. Fernandez, Anal. Chem. 82 (2010) 2178–2181.
[13] J.L. Zhang, Z.G. Zhou, J.W. Yang, W. Zhang, Y. Bai, H.W. Liu, Anal. Chem. 84 (2012) 1496–1503.
[14] J.L. Zhang, Z. Li, C.S. Zhang, B.S. Feng, Z.G. Zhou, Y. Bai, H.W. Liu, Anal. Chem. 84 (2012) 3296–3301.
[15] M.Z. Huang, S.S. Jhang, C.N. Cheng, S.C. Cheng, J. Shiea, Analyst 135 (2010) 759–766.
[16] J.S. Sampson, A.M. Hawkridge, D.C. Muddiman, J. Am. Soc. Mass Spectrom. 17 (2006) 1712–1716.
[17] K.S. Novoselov, A.K. Geim, S.V. Morozov, D. Jiang, Y. Zhang, S.V. Dubonos, I.V. Grigorieva, A.A. Firsov, Science 306 (2004) 666–669.
[18] C.N.R. Rao, A.K. Sood, K.S. Subrahmanyam, A. Govindaraj, Angew. Chem. Int. Edn. 48 (2009) 7752–7777.
[19] D.S. Li, W. Windl, N.P. Padture, Adv. Mater. 21 (2009) 1243.
[20] C. Berger, Z.M. Song, X.B. Li, X.S. Wu, N. Brown, C. Naud, D. Mayou, T.B. Li, J. Hass, A.N. Marchenkov, E.H. Conrad, P.N. First, W.A. de Heer, Science 312 (2006) 1191–1196.
[21] M.J. Allen, V.C. Tung, L. Gomez, Z. Xu, L.M. Chen, K.S. Nelson, C.W. Zhou, R.B. Kaner, Y. Yang, Adv. Mater. 21 (2009) 2098–2102.
[22] X.L. Dong, J.S. Cheng, J.H. Li, Y.S. Wang, Anal. Chem. 82 (2010) 6208–6214.
[23] M.H. Lu, Y.Q. Lai, G.N. Chen, Z.W. Cai, Anal. Chem. 83 (2011) 3161–3169.
[24] J. Zhang, X.L. Dong, J.S. Cheng, J.H. Li, Y.S. Wang, J. Am. Soc. Mass Spectrom. 22 (2011) 1294–1298.
[25] X.Z. Zhou, Y.Y. Wei, Q.Y. He, F. Boey, Q.C. Zhang, H. Zhang, Chem. Commun. 46 (2010) 6974–6976.
[26] Y.K. Kim, H.K. Na, S.J. Kwack, S.R. Ryoo, Y. Lee, S. Hong, Y. Jeong, D.H. Min, ACS Nano 5 (2011) 4550–4561.
[27] Y. Liu, J.Y. Liu, C.H. Deng, X.M. Zhang, Rapid Commun. Mass Spectrom. 25 (2011) 3223–3234.
[28] O.C. Compton, S.T. Nguyen, Small 6 (2010) 711–723.
[29] L.A.L. Tang, J.Z. Wang, K.P. Loh, J. Am. Chem. Soc. 132 (2010) 10976–10977.
[30] J.L. Chen, X.P. Yan, K. Meng, S.F. Wang, Anal. Chem. 83 (2011) 8787–8793.